Petroleum Science 19 (2022) 509–517

Contents lists available at ScienceDirect

Petroleum Science

journal homepage: www.keaipublishing.com/en/journals/petroleum-science

Original Paper

Porosity of gas shale: Is the NMR-based measurement reliable?

Peng Zhao [a], Bo He [b], Bo Zhang [c], Jun Liu [b, *]

[a] Key Laboratory of Deep Underground Science and Engineering (Ministry of Education), College of Architecture and Environment, Sichuan University, Chengdu, Sichuan 610065, China
[b] Institute of New Energy and Low-Carbon Technology, Sichuan University, Chengdu, Sichuan 610065, China
[c] Institute of Science and Technology, China Three Gorges Corporation, Beijing, 100038, China

ARTICLE INFO

Article history:
Received 16 March 2021
Accepted 26 September 2021
Available online 10 December 2021

Edited by Jie Hao

Keywords:
Gas shale
Low-field NMR
Porosity measurement
Low-temperature nitrogen adsorption

ABSTRACT

Aiming at obtaining an accurate porosity of gas shale, various approaches are attempted. Therein, nuclear magnetic resonance (NMR), being treated as a kind of new-developed technique, possesses the representative significance. However, as a booming technique, the reliability of NMR-based porosity of shale is not exactly defined. Depending on NMR device, this work measured the porosity of shale experiencing different water soaking time, accordingly, judging the reliability of NMR-based porosity. Results indicate the NMR outcomes vary with the water soaking time, making a doubt about the objectivity of NMR-based porosity in reflecting the real shale porosity. Furthermore, some supplementary means were adopted to verify the water soaking-induced variation in the pore system of shale sample, which intensities the suspicion if the NMR-based porosity is reliable or not. To sum up, this work considers that the NMR-based porosity of shale is not reliable enough when water is used as the probe. Besides, this work also offers some suggestions on how to enhance the reliability of NMR-based porosity of shale sample. Basically, this work selects a fresh perspective to analyze the NMR approach in determining shale porosity, which is hopefully helpful in promoting the development of NMR technique in the shale-related field.

1. Introduction

In recent decades, with rising international concerns over the huge demand of energy resources, significant emphasis on the development of shale gas has sparked much attention all over the world (Liu et al., 2017b, 2021; Zhou et al., 2019). Under this background, current knowledge strongly supports that porosity is a crucial parameter for the shale gas exploration and exploitation, because the pore space is of great significance for the gas storage in shale reservoir (Sheng et al., 2019; Huang et al., 2020). Therefore, a precise porosity measurement plays an irreplaceable role in the responsible development of shale gas, including the selection of favorable section, the estimation of gas resources, and the design of production strategy, etc. (Huang et al., 2020; Tian et al., 2020). Accordingly, how to obtain a reliable shale porosity has attracted significant recent attention, serving for an expanding understanding on the tight shale reservoir and the gas stored in it.

Basically, the frequently-used methodologies aiming to get the shale porosity can be subdivided into two categories. One is called as the physical testing, which employs a probe (e.g., gas/water) to detect the pore space of shale, while the another is the imaging analysis and is a direct approach to observe the pore topography of shale samples by using an auxiliary equipment like microscope (Li et al., 2019; Huang et al., 2020). In general, the physical method usually includes the helium pycnometry (HP), low-temperature nitrogen adsorption (LTNA), carbon dioxide (CO_2) adsorption, mercury intrusion porosimetry (MIP), and nuclear magnetic resonance (NMR), while the imaging methodology mainly contains scanning electron microscopy (SEM), transmission electron microscopy (TEM), and X-ray computed tomography (CT) (Zhao et al., 2018; Huang et al., 2020; Ma et al., 2020). As far as these mentioned approaches above, the resolution is variable and each one has its individual personality —simple or complicated operation, less or long time-used, and low- or high-cost, etc. For example, the CT technique is able to exhibit the shale pore system in a 3D manner, but usually has a relative lower resolution (Wang et al., 2016). One more example, the LTNA approach is simple to operate, but is

* Corresponding author.
E-mail address: j.liu@scu.edu.cn (J. Liu).

https://doi.org/10.1016/j.petsci.2021.12.013

basically time-consuming (roughly a week for a measurement period) (Liu et al., 2018a; Zhao et al., 2018).

Among the approaches of shale porosity test, the NMR technique, based on the liquid-state ^{1}H NMR relaxation, becomes popular in more recent years, since it is regarded as a fast, convenient and non-destructive method for characterizing the pore information of shale, including the porosity, pore geometry, and pore connectivity, etc. (Yao and Liu, 2012; Yao et al., 2014; Li et al., 2015, 2017, 2018; Liu et al., 2018b, 2020a, 2020b). Li et al. (2017) characterized the pore size types of the shale samples from the Lower Cambrian Qiongzhusi Formation (Sichuan Basin, China), which revealed the residual porosity and movable porosity depending on the transverse relaxation time (T_2) spectrum. Xu et al. (2015) compared the porosity measured by NMR technique and HP approach and found the He porosity is larger than the NMR porosity. Comparatively, Adeyilola et al. (2020) stated that the porosity values from NMR measurement were higher than those from HP method, using the shale samples from the Lower Bakken formation (North Dakota). It's not hard to see there is a tendency that the position of NMR method is increasingly prominent in the research related to shale porosity. During the NMR measurement, distilled water or brine is usually employed as the probe in characterizing the porosity of gas shale (Xu et al., 2015; Li et al., 2017; Adeyilola et al., 2020). However, the clay minerals, considerably existing in shale, have a great influence on the porosity results from the NMR measurement — a water-based methodology. Accordingly, Yan et al. (2018) put forward a method and tried to make the NMR-based porosity more accurate, by choosing the magic-sandwich echo (MSE) pulse sequence rather than the Carr-Purcell-Meiboom-Gill (CPMG) pulse sequence during the NMR operation. Nevertheless, there is a reasonable doubt that whether the NMR-based porosity itself is reliable or not, in view of some inconsistencies exist in the NMR-related works. For example, which one of the NMR method and Helium porosimetry tends to enable a greater porosity value (Xu et al., 2015; Adeyilola et al., 2020)?

As a result, the reliability of NMR application in characterizing shale porosity is worthy of a deepening study. In this work, to analyze the utility of NMR approach as a detective of the shale porosity, a series of experimental operations were conducted. Firstly, the NMR-based porosity was obtained after the involved shale sample experienced water soaking; then, the LTNA technique and CT scanning were employed as supplementary means to instruct whether the NMR measurement of shale porosity is reliable or not. Under the circumstance that NMR technique is widely introduced in the petrophysical characterization of shale, this work raises a question about the reliability of NMR-based porosity, aiming to offer a change of perspective on this technique. This work is expected to be helpful in promoting the development of NMR technique in the characterization of shale porosity.

2. Materials and analytical methodology

2.1. Sampling and pretreatment

A total of four shale samples were obtained from a shale gas well located in Yibin City, a hotspot for Chinese shale gas industry in Sichuan basin, SW China. Characterized as carbonaceous shale, all the core samples belong to the lower Silurian Longmaxi formation which is the main target stratum for the commercial development of Chinese shale gas so far (Liu et al., 2017b; Zhang et al., 2020), indicating the collected samples are representative. Listed in Table 1, the basic properties of collected samples were determined using the methods shown by Liu et al. (2019b), like the X-ray diffraction (XRD) for mineral examination, the carbon sulfur for total organic carbon (TOC) test, and Langmuir theory for CH_4 adsorption. Basically, minerals in the sample are dominated by quartz and clay minerals, conforming to the mineral composition characteristic of the typical marine shale. The shale samples have high content of TOC and high thermal maturity (reflected by vitrinite reflectance, R_o). Besides, the excess adsorption capacity (revealed by Langmuir volume, V_L) for CH_4 of all samples is impressive and indicates the great potential of shale gas resources in sampling well.

In this work, each collected shale sample was processed into cylinders with a length of 10 mm and a diameter of 10 mm for the NMR tests and CT scanning, relying on the diamond wire cutting and processing technology. Then, the cuttings were grinded into fragments with a size of roughly 1–2 mm, preparing for the LTNA measurements.

2.2. NMR measurement

2.2.1. NMR theory in porosity characterization

The NMR behavior is sensitive to the hydrogen protons of fluids in shale pores, called spins, where the number of hydrogen atoms present in the ^{1}H-fluid can be reflected according to the T_2 measurement (Seevers, 1966). This principle has performed very well in many previous studies (Yao et al., 2010; Liu et al., 2017a, 2019a; Zheng et al., 2018). Basically, current achievements have verified that the behavior of the NMR signal is related to the various surrounding environments for the ^{1}H-fluid, so the detected T_2 reflects the mobility of the ^{1}H-molecules and correlates with pore size (Yao et al., 2010; Li et al., 2017; Liu et al., 2018b, 2020b; Huang et al., 2020):

$$\frac{1}{T_2} = \rho_2 \left(\frac{S}{V}\right) \tag{1}$$

where ρ_2 is the surface relaxivity and S/V is the surface-to-volume ratio of the pore. Accordingly, the resulting T_2 positively correlates to the pore radius, that is, a shorter T_2 is indicative of a smaller pore radius.

2.2.2. NMR-based scheme

The NMR experiments were performed using a GeoSpec 2/150 low-field NMR spectrometer (Oxford DRX HF with Q-SENSE), operating at a resonant frequency of ~2.5 MHz. During the NMR operations, the experiment temperature remains constant at 30 °C. Besides, other key settings parameters of NMR detector, including T_2 maximum number of echoes of 10,000; echo interval of 0.12 ms, waiting time of 3500 ms, and scan times of 64, were set for capturing the maximum recovery of the polarized NMR T_2 signal and the fast relaxation components.

Before the NMR measurement, each prepared sample was dried in a vacuum oven for 24 h and then was fully saturated with distilled water for 2 days (48 h). At this juncture, the NMR test was conducted. After the NMR test, the sample continued to be immersed in distilled water for another 5 days, enabling the water soaking time of each reaches to 7 days (168 h) in total; at this point, the second NMR test was performed. During each NMR measurement, the T_2 spectra were recorded automatically. In an intelligent manner, the built-in program/algorithm of NMR apparatus during the measurement enables three outputs: 1) NMR Total Porosity: The total area under the 100% saturated T_2 distribution; 2) Clay Bound Water: The area of the connate water T_2 distribution up to the clay bound cut-off entered (usually 2.5 msec); 3) Effective porosity: The total porosity minus the clay bound water. The NMR apparatus and theory (e.g., the boundary time value of 2.5 msec) used in this work are the same with the ones employed by Huang et al. (2020) and Ai et al. (2021).

Table 1
Basic properties of the shale samples in this work.

Sample ID	Buried depth, m	Mineral composition, wt%					TOC, %	R_o, %	V_L, m^3/t	He porosity, %
		Quartz	Clay minerals	Feldspar	Carbonate minerals	Pyrite				
Sample A	4142	47.5	23.4	7.1	20.5	1.5	2.72	2.31	2.61	2.42
Sample B	4125	46.2	27.3	8.8	15.5	2.2	2.23	2.40	2.37	2.81
Sample C	4128	51.1	17.8	10.5	17.4	3.2	3.21	2.23	2.44	4.26
Sample D	4230	47.6	19.9	6.7	23.2	2.6	3.86	3.41	2.93	3.15

Note: TOC, total organic carbon; R_o, vitrinite reflectance; V_L, Langmuir volume (measured at 30 °C with pressures up to 11 MPa).

2.3. Supplementary means

In this work, LTNA and CT techniques are employed to get the supporting information for the judgement on the reliability of NMR-based porosity of gas shale. Herein, these two approaches are mainly pay attention to the (possible) variation of shale pore system during the water saturation – LTNA works from the micro-perspective and CT performs from the macro-perspective (resolution of ~8 μm).

2.3.1. LTNA measurement

LTNA is a mature technique in characterizing the rock pore system, such as coal, silicate and sandstone (Kelemen and Kwiatek, 2009; Alam and Mokaya, 2015; Xu et al., 2018), as well as in providing reliable reflection of gas shale on the pore type, pore size distribution (PSD), and pore volume, etc. (Chen et al., 2017, 2018; Liu et al., 2018a; Zhao et al., 2018). In this work, each sample was experienced two times of LTNA measurement: before water involvement and after water soaking for 7 days (168 h). Prior to the LTNA test, the prepared sample was fully dried until it was weighted with an unchanged quality. Then, at the temperature of 77 K, the N_2 adsorption isotherms were obtained with the relative pressure (P/P_0) ranging from 0.01 to 0.995, using the ASAP 2460 instrument with the built-in MicroActive software. Accordingly, the specific surface area (SSA) was obtained by the Brunauer-Emmette-Teller (BET) model, while the pore volume and pore diameter were analyzed with the Barrette-Joynere-Halenda (BJH) and density functional theory (DFT) methods.

2.3.2. CT scanning

The CT scanning was conducted following the NMR test, which can recognize the internal fractures of the shale samples in the nondestructive status. In this work, the employed industrial CT is type of V|tome|xL300 and made by GE Sensing & Inspection Technologies Gmbh. Depending on this CT scanner, both the columnar samples of Sample B and Sample D were scanned twice – before water soaking and after 7 days water soaking, aiming to visualize the natural fractures inner shale sample. To maximize the accuracy of CT scanning outputs, the main parameters were set as follows: scanning voltage of 150 kV, scanning current of 150 μA, and resolution ratio of ~8 μm.

Subsequent to the CT scanning, an image processing software called Mimics was employed to manage the CT outputs, by which the fracture morphology, orientation and spatial distribution of the internal fractures are able to be characterized in a 3D manner. Accordingly, the CT images were processed and located, relying on the principle that the shale matrix and fracture have different thresholds, in order to facilitate the extraction of the shale matrix and fracture within the samples. This similar Mimics-related approach in dealing with CT scanned images was successfully exhibited in Jiang et al. (2019).

3. Results and discussion

In this work, the NMR performances of each sample after experiencing different water soaking time were compared first; then the LTNA and 3D CT outputs were also compared for every sample, aiming to explore the (possible) influence of water soaking on the pore system of shale. Thereafter, the uncertainty and reliability of NMR-based porosity of gas shale are discussed.

3.1. NMR performance and measured porosity of gas shale

Similar to previous achievements (Li et al., 2017; Liu et al., 2020a), the NMR amplitudes of shale samples mainly are of bimodal type, supplemented with a few trimodal type (Fig. 1). For all measured NMR T_2 spectrums, there is a common ground that the most obvious peak is the far left one that is in a short relaxation time normally peaked at 0.01–10 ms. This phenomenon indicates the pores in shale are mainly characterized as considerably small, according to Eq. (1). For every sample, it is found that the NMR amplitude for 2 days water soaking differs from that for 7 days water soaking. For example, the two peaks are connected at 2 days water soaking and become isolated at 7 days water soaking for Sample A (Fig. 1a), while the situation for Sample B (Fig. 1b) is just opposite with that for Sample A. This is mainly to the different variations which occur to the pore system of these two samples. Referring from Li et al. (2017), the continuous and discontinuous NMR T_2 spectrum correspond to a good and poor connectivity between small pores and large pores in shale, respectively. Therefore, it could be speculated that the communication paths between pores in different size probably have changed during the water soaking process.

Derived from the NMR measurements, the outputs including the total NMR porosity, the clay bound water and the effective porosity vary when the water soaking is conducted for different time (Fig. 2), where there seems to be no uniform law in the variation behavior and change rate. Herein, for Samples A and C, the 7 days water soaking makes the total NMR porosity and the clay bound water experience a decline, compared the situations at 2 days water soaking (Fig. 2a and b). Besides, a longer water soaking enables an soft increase of the effective porosity for all samples (except for Sample B) (Fig. 2c). Per the statistics, compared to a shorter water soaking (2 days), a longer one (7 days) bring a change rate of −6% ~29%, −8%~33% and −4%~12% in the total NMR porosity, the clay bound water and the effective porosity (Fig. 2). This phenomenon indicates the various degrees of variation objectively exist in all the NMR outputs, when the shale sample experiences a longer water soaking time. That is to say, the water soaking behavior is probably able to induce some alterations in the NMR-based porosity of shale samples, possibly bringing some uncertainties when NMR approach is adopted in measuring the shale porosity.

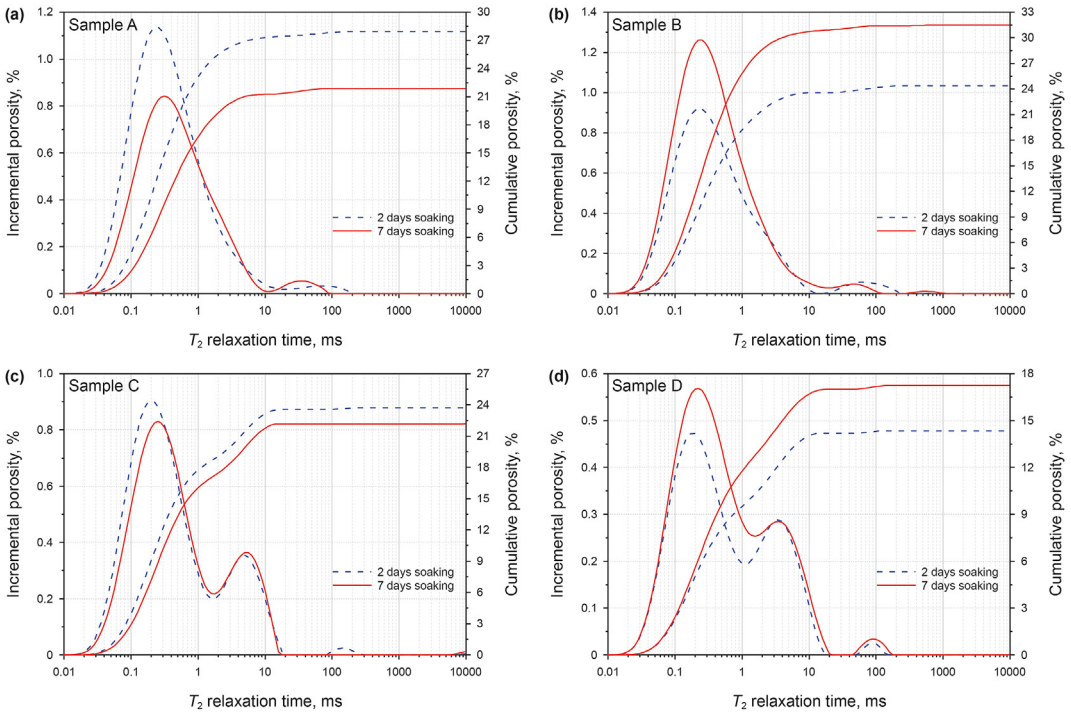

Fig. 1. NMR T_2 spectrums of shale samples after experiencing different water soaking time.

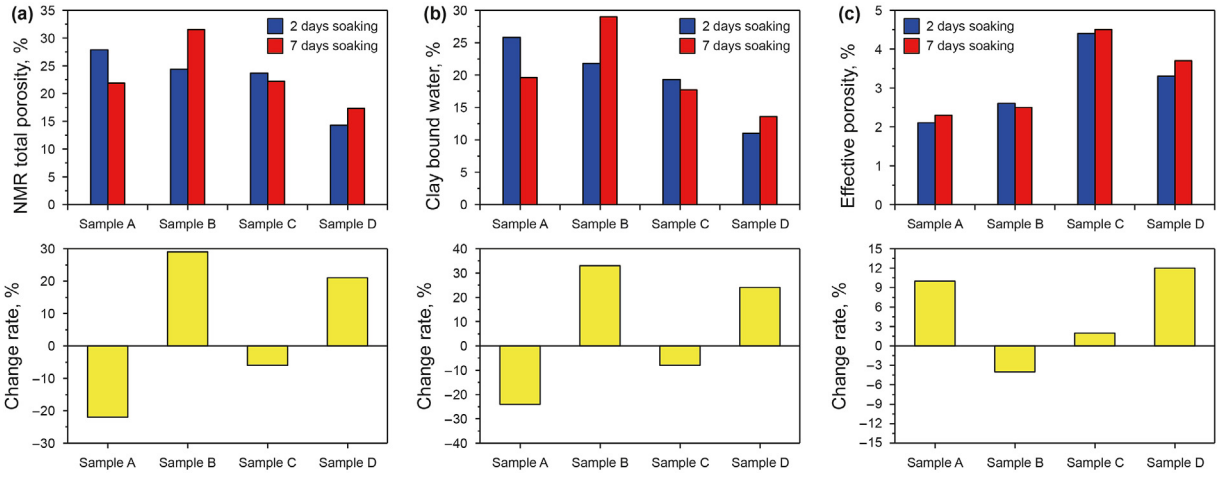

Fig. 2. NMR total porosity (a), clay bound water (b), effective porosity (c) and their change rate of shale samples after experiencing different water soaking time.

3.2. Pore system analysis from the LTNA measurement and CT scanning

Although the variations in the NMR-based outputs are observed (Figs. 1 and 2), admittedly these NMR-related phenomena are inadequate to account for the judgement if the NMR-based porosity is reliable or not. Therefore, the LTNA is introduced by this work, aiming to provide a more insightful perspective on the reliability of NMR-based porosity. Fig. 3 exhibits the N_2 gas adsorption–desorption isotherms of all study samples, where these isotherms are characterized as Type IV, with noticeable hysteresis loops, according to the International Union of Pure and Applied Chemistry (IUPAC) classification (Liu et al., 2018a). Thereinto, it is reported that the presence of hysteresis implies the evaporation from pores is a distinctly different process than the condensation within the pores (Sing, 1985). In Fig. 3, for all the LTNA measurements, a 'sudden drop' of desorption branch emerged at $P/P_0 = \sim 0.5$, called as the Tensile Strength Effect (Groen et al., 2003). Besides, based on the implications of hysteresis loop shape (Sing, 1985), the pore type of all the samples (before and after water soaking) are of H2 (inkbottle-shaped pore) — the pores with narrow necks and wide bodies. However, by comparison, whether the water soaking is conducted or not enables the different process of adsorption/desorption in the LTNA measurements for each shale sample (Fig. 3). For example, compared to the situation without water soaking, 7 days water soaking makes the quantity adsorbed inferior and superior for the Sample A and Sample C, respectively, in both the adsorption and desorption processes (Fig. 3). However, more attentions are needed to explain the reason for the differential variations among samples emerging to the nitrogen adsorption and

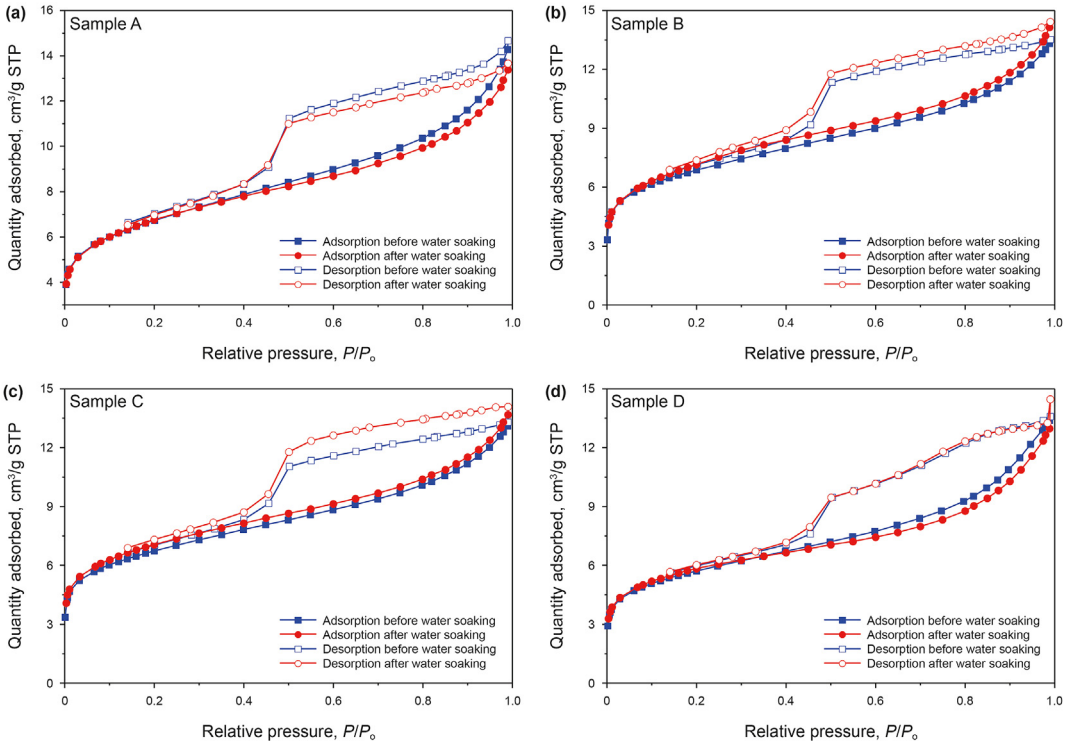

Fig. 3. Nitrogen adsorption–desorption isotherms of shale samples before and after water soaking treatment.

desorption process, in the water soaking process.

Due to the variation in the adsorption/desorption process, the LTNA outcomes after water soaking differ from those without water soaking to some degree (Fig. 4). These differences happen to BET area surface, BJH adsorption/desorption pore volume, BJH adsorption/desorption average pore width, and DFT total pore volume. For example, compared to the status without water involvement, the 7 days water soaking enables the BJH adsorption pore volume of Sample A and Sample B to be smaller and greater, respectively (Fig. 4b). Indeed, some parameters (e.g., the BET surface of Sample A) do not experience an obvious change after being soaked in water, but the water soaking-induced variation has really happened to at least one index for each sample in a discernible manner, as shown in Fig. 4.

In addition, the 7 water soaking also stimulates some variations to the performances of the PSD and the pore volume/surface at different pore width (Figs. 5, 6 and7). Overall, the variations emerging to Sample A and Sample B are more apparent, possibly resulted from the relatively greater content of clay minerals in Sample A and Sample B than the rest two samples, according to Yan et al. (2018). Moreover, the LTNA outcomes also indicate that all the variations seem to happen to the pores with a width smaller than 30 nm (mainly <10 nm) (Figs. 5, 6 and 7), suggesting the water soaking operation sparingly affects the pores with a bigger size.

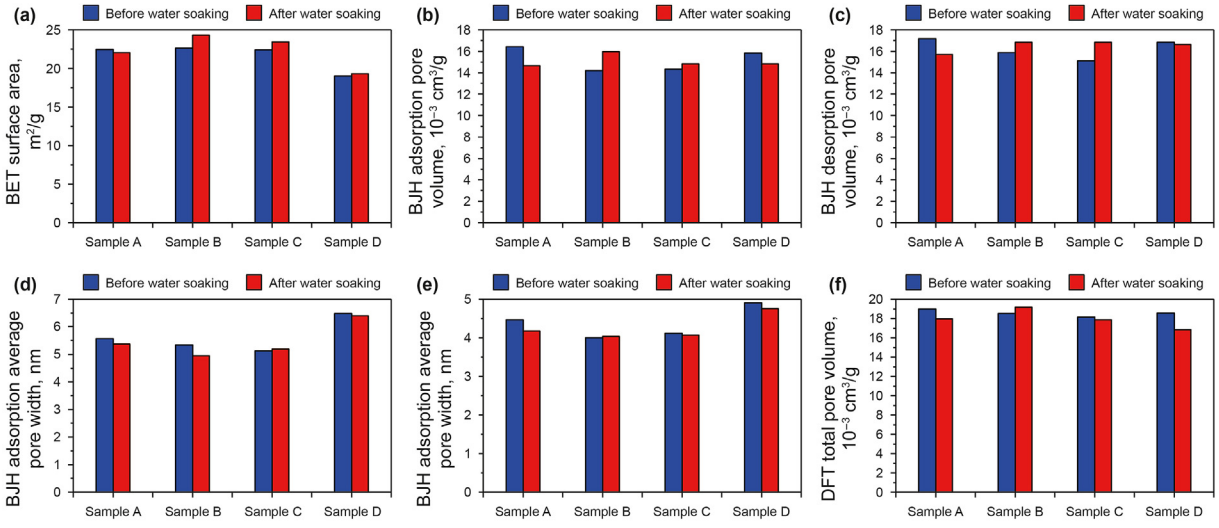

Fig. 4. LTNA-based outcomes about the pore system of shale samples before and after water soaking.

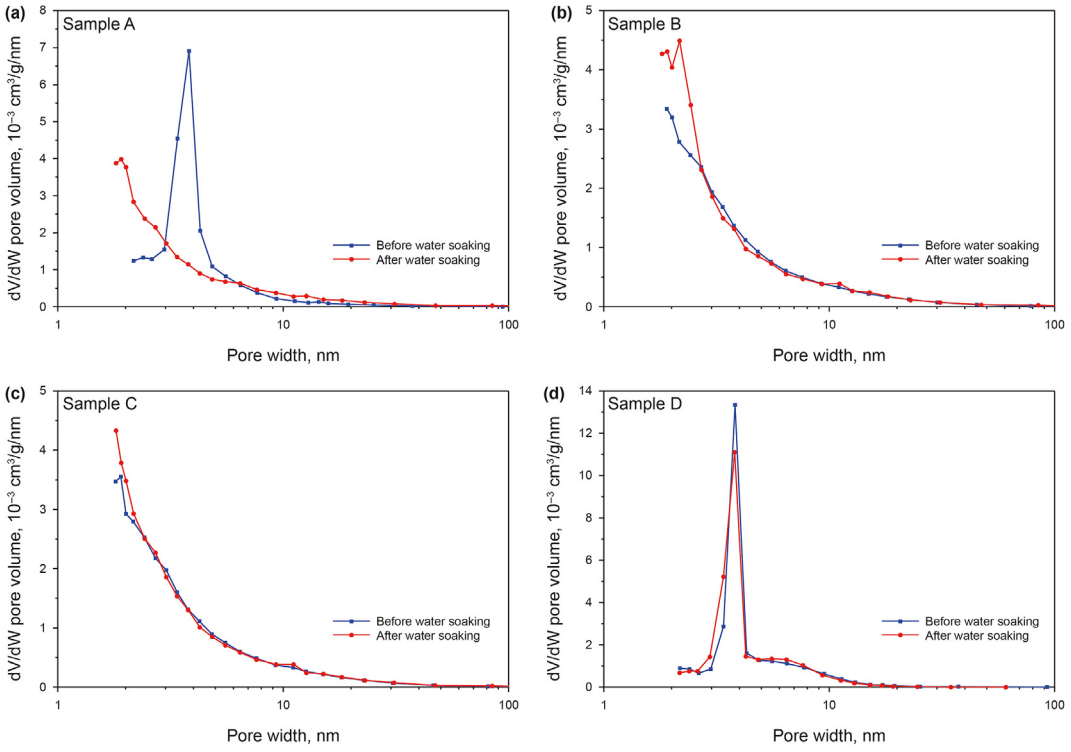

Fig. 5. PSD performance of study samples before and after water soaking.

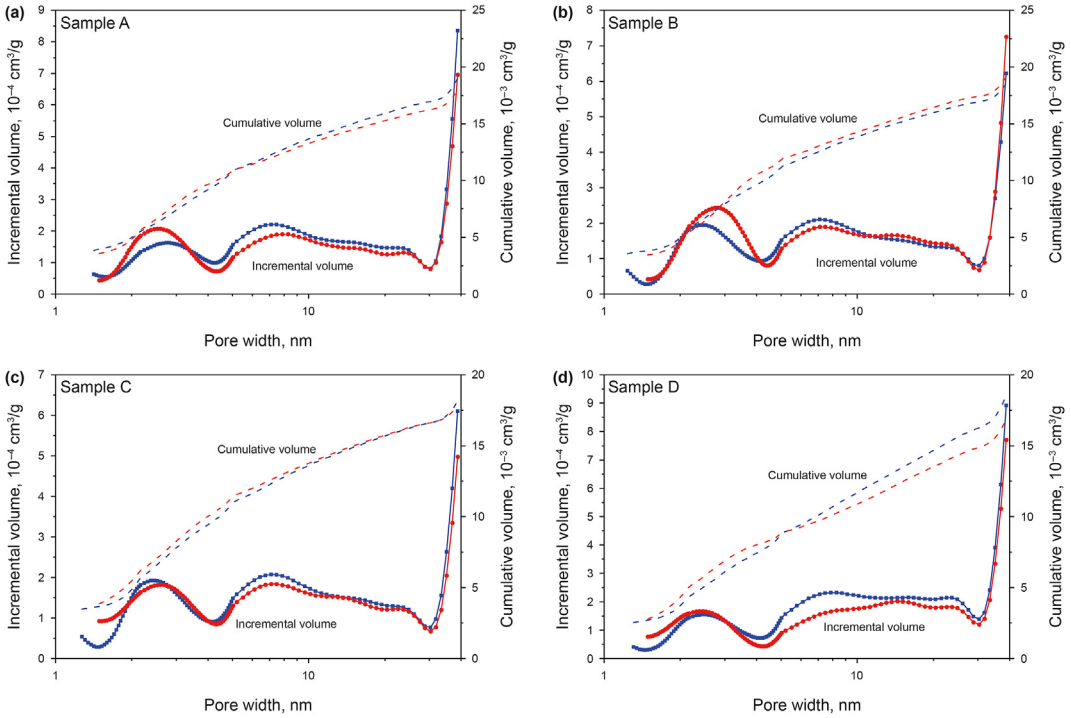

Fig. 6. Pore volume of study shale samples. The blue and red series represent the situation without and with water soaking, respectively.

To explore if the water soaking induces a variation to the fracture system in shale sample, the CT scanning is adopted in this work and is exhibited in Fig. 8. By contrast, imperceptible changes have happened to the samples after being soaked in water for 7 days. This phenomenon further echoes the LTNA-based summary that water soaking almost has no influence in the pores in big size. That is to say, the observed variations, from both NMR and LTNA approaches, have connection with small pores.

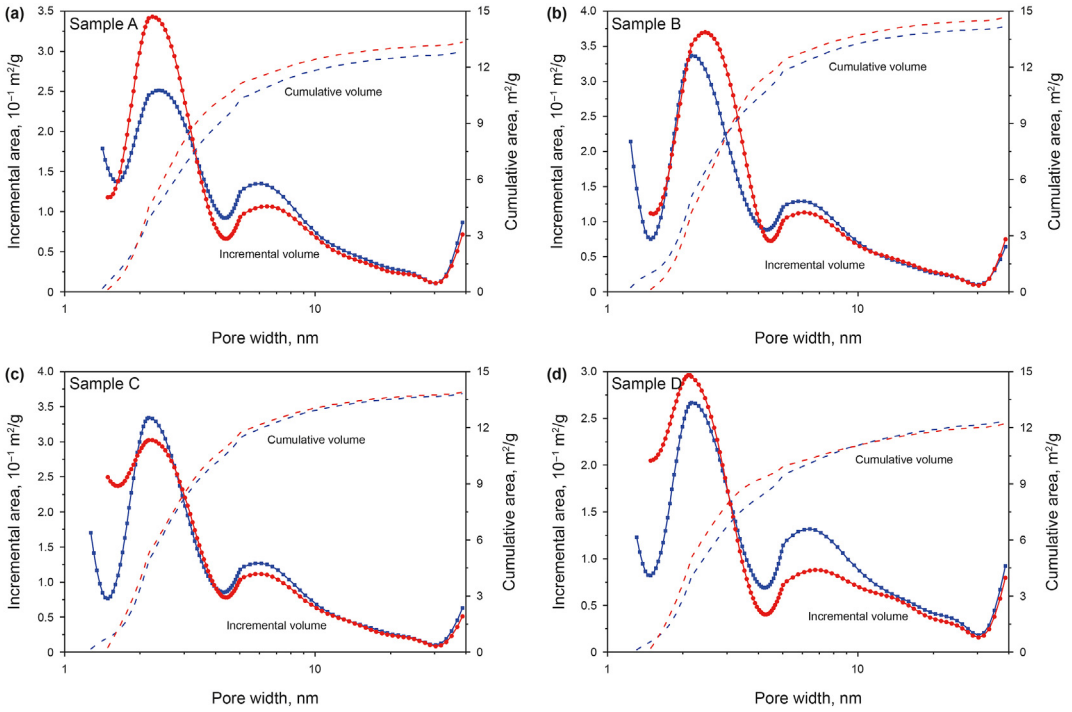

Fig. 7. Surface area of study shale samples. The blue and red series represent the situation without and with water soaking, respectively.

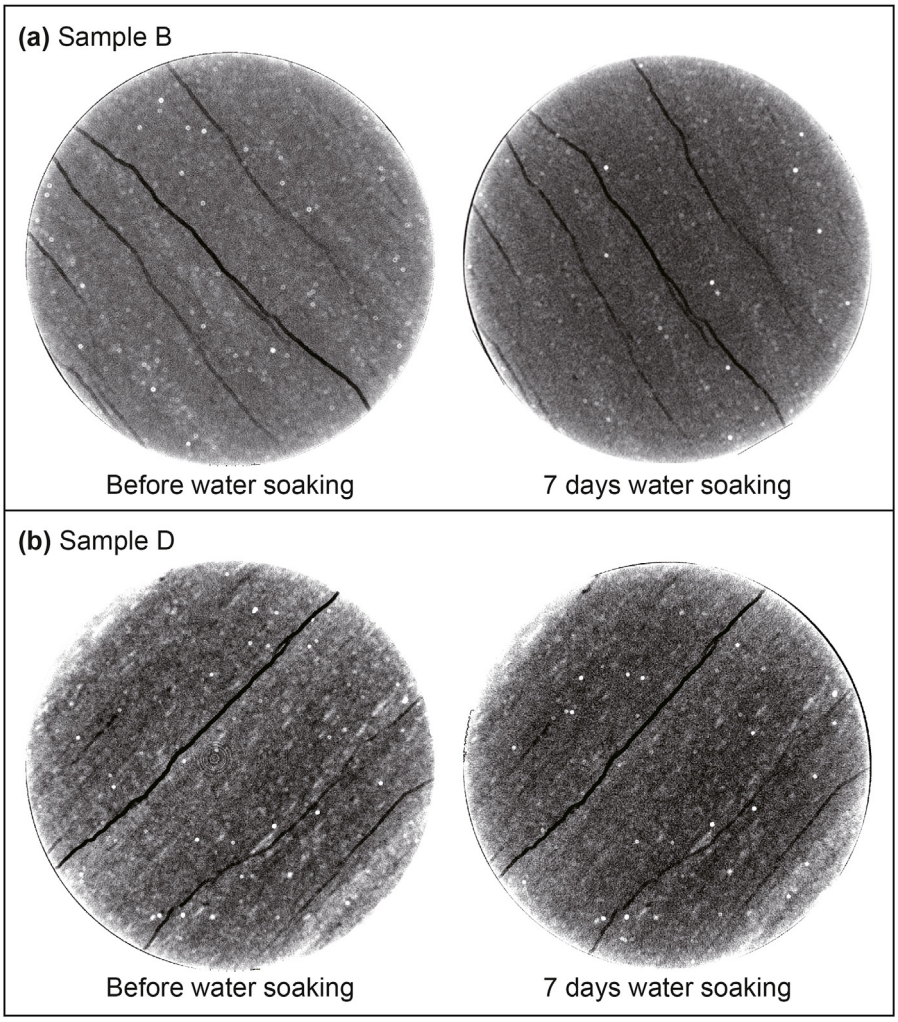

Fig. 8. Internal fractures of shale samples exhibited by CT scanning. Diameter of each slide is 10 mm.

3.3. Uncertainty of NMR-based porosity of gas shale

Now that the water soaking-induced variation in the pore system in shale is observed by NMR method and is verified by other supplementary means, it is needed to consider the reliability of the NMR-based porosity of shale when water is involved in this NMR measurement. In other words, it is worth considering that if the NMR-based porosity with water soaking being adopted can represent the real porosity of shale. This is because that the shale sample after being soaking in water for a certain time is no longer the one it used to be (before water soaking), where pore system has been changed to some degree, exhibited by the NMR and LTNA results. This is probably the reason why Xu et al. (2015) and Adeyilola et al. (2020) reported an opposite opinion on the comparison between porosities from He porosimetry method and NMR approach.

The water soaking-induced variation in shale pore system is mainly attributed to capillary hydration and surface-osmotic hydration (Roshan et al., 2015), which is accepted by Huang et al. (2020) to explain why shale decomposition happens during the water soaking process, and its essence is the variation experienced by shale pore system. In this work, the hydration effect is also supposed to be the primary cause for the pore system variation induced by water soaking. Besides, the pore water in shale usually occurs in adsorbed and free states, and the ratios of adsorbed and free water depend on the size and morphology of pores for certain state parameters (Li et al., 2019). And, the water soaking time may also affect the proportion or/and content of adsorbed and free water, which possibly affects the NMR porosity results as well. Accordingly, there are two doubts about the NMR measurement: 1) can the NMR-based porosity with water involvement represent the porosity of shale sample before water soaking? 2) what is the maximum duration for water soaking time to keep the NMR-based porosity within an acceptable error bound? Prior to addressing these issues, the reliability of the NMR-based porosity of gas shale should be greeted with doubt when water soaking is involved in this measurement process.

It is worth noting that the influence of water soaking on the pore system has attracted increasing attentions, even for the pore system of coal rock. Ai et al. (2021) organized a series of water soaking operations (3 h, 6 h, 12 h, 24 h, 36 h, 2 d, 4 d, 10 d, and 20 d) on coal rock, and grabbed the relationship between the water soaking time and the average pore size. This also indirectly indicates that the NMR-based porosity has some uncertainties when it used as the porosity of rock sample (e.g., shale and coal), as water is usually used as a probe in this measurement.

4. Conclusions

In this work, the reliability of NMR-based porosity is analyzed, depending on the porosity measurements on the shale sample experiencing different water soaking time. This analysis is supported by the LTNA and CT approaches. Accordingly, the main conclusions are made.

It is undeniable that NMR measurement has the ability to provide a porosity value of shale soaking with water, and to reveal the PSD information as well. However, a shale sample has a variable NMR-based porosity value when the water soaking time varies, leading to a doubt that if the NMR measurement with water involvement can objectively and impartially reflect the real porosity of a shale sample or not.

The LTNA and CT measurements assuredly illustrate the water soaking-induced variations in the internal pores in shale, such as the BET surface area, BJH adsorption/desorption pore volume and PSD, where these variations tend to happen to the pores with small size (usually <30 nm). Against these variations, the reliability of NMR-based porosity is further questioned, when water is selected as the probe in the NMR methodology. Additionally, maybe an NMR-based standard for the NMR measurement for gas shale porosity could be explored to guide the related operation, if water is involved in this process.

To enhance the reliability of NMR-based porosity of gas shale, this work suggests the future investigations on 1) how to enable the NMR-based porosity to render into the porosity of shale sample before water soaking? 2) how to make a regulation for the water soaking operation to enable the NMR-porosity of shale sample to locate within the error allowed? Besides, this work also suggests that 1) waterless probe could be taken into consideration to avoid the pore system variation existing in the process of the water-based sample preparation and that 2) aqueous solution (like salt water) could be used to avoid the water sensitive effect that usually happens to clay minerals in shale, when NMR-based porosity is measured.

Conflicts of interest

The authors declare that they have no known competing financial interests or personal relationships that could influence the work reported in this paper.

Acknowledgements

This study was financially supported by the Science and Technology Department of Sichuan Province (Grant Nos. 2021YFH0048 and 2021YFH0118), and the Project funded by China Postdoctoral Science Foundation (Grant No. 2020M683253). The authors would like to thank Dr. Yingming Zhu from Institute of New Energy and Low-Carbon Technology of Sichuan University for his help with experimental operations of CT scanning.

References

Adeyilola, A., Nordeng, S., Onwumelu, C., et al., 2020. Geochemical, petrographic and petrophysical characterization of the lower bakken shale, divide county, north Dakota. Int. J. Coal Geol. 224, 103477. https://doi.org/10.1016/j.coal.2020.103477.

Ai, T., Wu, S., Zhang, R., et al., 2021. Changes in the structure and mechanical properties of a typical coal induced by water immersion. Int. J. Rock Mech. Min. 138, 104597. https://doi.org/10.1016/j.ijrmms.2020.104597.

Alam, N., Mokaya, R., 2015. Strongly acidic mesoporous aluminosilicates prepared via hydrothermal restructuring of a crystalline layered silicate. J. Mater. Chem. A. 3 (15), 7799–7809. https://doi.org/10.1039/c5ta00548e.

Chen, F.W., Ding, X., Lu, S.F., et al., 2017. The pore characterization of the lower silurian Longmaxi shale in the southeast chongqing, China using FE-SEM, LTNA and MIP methods. J. Nanosci. Nanotechnol. 17 (9), 6482–6488. https://doi.org/10.1166/jnn.2017.14406.

Chen, F.W., Lu, S.F., Ding, X., et al., 2018. The splicing of backscattered scanning electron microscopy method used on evaluation of microscopic pore characteristics in shale sample and compared with results from other methods. J. Petrol. Sci. Eng. 160, 207–218. https://doi.org/10.1016/j.petrol.2017.10.063.

Groen, J.C., Peffer, L.A.A., Perez-Ramírez, J., 2003. Pore size determination in modified micro- and mesoporous materials. Pitfalls and limitations in gas adsorption data analysis. Microporous Mesoporous Mater. 60 (1–3), 1–17. https://doi.org/10.1016/S1387-1811(03)00339-1.

Huang, Z.Q., Zhang, Y., Xie, L.Z., et al., 2020. Comparative study of porosity test methods for shale. Arab. J. Geosci. 13 (2), 94. https://doi.org/10.1007/s12517-020-5086-5.

Jiang, C.B., Niu, B.W., Yin, G.Z., et al., 2019. CT-based 3D reconstruction of the geometry and propagation of hydraulic fracturing in shale. J. Petrol. Sci. Eng. 179, 899–911. https://doi.org/10.1016/j.petrol.2019.04.103.

Kelemen, S.R., Kwiatek, L.M., 2009. Physical properties of selected block Argonne Premium bituminous coal related to CO_2, CH_4, and N_2 adsorption. Int. J. Coal Geol. 77 (1–2), 2–9. https://doi.org/10.1016/j.coal.2008.05.020.

Li, A., Ding, W.L., Wang, R.Y., et al., 2017. Petrophysical characterization of shale reservoir based on nuclear magnetic resonance (NMR) experiment: a case study of Lower Cambrian Qiongzhusi Formation in eastern Yunnan Province, South China. J. Nat. Gas Sci. Eng. 37, 29–38. https://doi.org/10.1016/j.jngse.2016.11.034.

Li, J.J., Yin, J.X., Zhang, Y.N., et al., 2015. A comparison of experimental methods for describing shale pore features - a case study in the Bohai Bay Basin of eastern China. Int. J. Coal Geol. 152, 39–49.

Li, J.Q., Wang, S.Y., Lu, S.F., et al., 2019. Microdistribution and mobility of water in gas

shale: a theoretical and experimental study. Mar. Petrol. Geol. 102, 496–507. https://doi.org/10.1016/j.coal.2015.10.009.
Li, X.C., Kang, Y.L., Haghighi, M., 2018. Investigation of pore size distributions of coals with different structures by nuclear magnetic resonance (NMR) and mercury intrusion porosimetry (MIP). Measurement 116, 122–128. https://doi.org/10.1016/j.measurement.2017.10.059.
Liu, J., Xie, L., Elsworth, D., et al., 2019a. CO_2/CH_4 competitive adsorption in shale: implications for enhancement in gas production and reduction in carbon emissions. Environ. Sci. Technol. 53 (15), 9328–9336. https://doi.org/10.1021/acs.est.9b02432.
Liu, J., Xie, L., He, B., et al., 2021. Influence of anisotropic and heterogeneous permeability coupled with in-situ stress on CO_2 sequestration with simultaneous enhanced gas recovery in shale: quantitative modeling and case study. Int. J. Greenh. Gas Con. 104, 103208. https://doi.org/10.1016/j.ijggc.2020.103208.
Liu, J., Xie, L., Yao, Y., et al., 2019b. Preliminary study of influence factors and estimation model of the enhanced gas recovery stimulated by carbon dioxide utilization in shale. ACS Sustain. Chem. Eng. 7 (24), 20114–20125. https://doi.org/10.1021/acssuschemeng.9b06005.
Liu, J., Yao, Y., Liu, D., et al., 2017a. Experimental evaluation of CO_2 enhanced recovery of adsorbed-gas from shale. Int. J. Coal Geol. 179, 211–218. https://doi.org/10.1016/j.coal.2017.06.006.
Liu, J., Yao, Y., Liu, D., et al., 2018a. Comparison of pore fractal characteristics between marine and continental shales. Fractals 26 (2), 1840016. https://doi.org/10.1142/S0218348X18400169.
Liu, J., Yao, Y., Liu, D., et al., 2017b. Comparison of three key marine shale reservoirs in the southeastern margin of the Sichuan basin, SW China. Minerals 7 (10), 179. https://doi.org/10.3390/min7100179.
Liu, X., Zhang, J., Bai, Y., et al., 2020a. Pore structure petrophysical characterization of the upper cretaceous oil shale from the songliao basin (NE China) using low-field NMR. J. Spectrosc. 2020, 1–11. https://doi.org/10.1155/2020/9067684.
Liu, Y., Yao, Y.B., Liu, D.M., et al., 2018b. Shale pore size classification: an NMR fluid typing method. Mar. Petrol. Geol. 96, 591–601. https://doi.org/10.1016/j.marpetgeo.2018.05.014.
Liu, Z.S., Liu, D.M., Cai, Y.D., et al., 2020b. Application of nuclear magnetic resonance (NMR) in coalbed methane and shale reservoirs: a review. Int.l J. of Coal Geol. 218, 103261. https://doi.org/10.1016/j.coal.2019.103261.
Ma, B.Y., Hu, Q.H., Yang, S.Y., et al., 2020. Multiple approaches to quantifying the effective porosity of lacustrine shale oil reservoirs in bohai bay basin, east China. Geofluids 2020, 8856620. https://doi.org/10.1155/2020/8856620.
Roshan, H., Ehsani, S., Marjo, C.E., et al., 2015. Mechanisms of water adsorption into partially saturated fractured shales: an experimental study. Fuel 159, 628–637. https://doi.org/10.1016/j.fuel.2015.07.015.
Seevers, D.O., 1966. A Nuclear Magnetic Method for Determining the Permeability of Sandstones, Paper L, SPWLA 7th Annual Logging Symposium. Society of Professional Well Log Analysts Transactions, Tulsa, Oklahoma, pp. 1–14.
Sheng, G.L., Javadpour, F., Su, Y.L., 2019. Dynamic porosity and apparent permeability in porous organic matter of shale gas reservoirs. Fuel 251, 341–351. https://doi.org/10.1016/j.fuel.2019.04.044.
Sing, K.S., 1985. Reporting physisorption data for gas/solid systems with special reference to the determination of surface area and porosity. Pure Appl. Chem. 57, 603–619. https://doi.org/10.1351/pac198557040603.
Tian, H., Zou, C., Liu, S., et al., 2020. Reservoir porosity measurement uncertainty and its influence on shale gas resource assessment. Acta Geol. Sin. 94 (2), 233–242. https://doi.org/10.1111/1755-6724.14287.
Wang, Y., Pu, J., Wang, L.H., et al., 2016. Characterization of typical 3D pore networks of Jiulaodong formation shale using nano-transmission X-ray microscopy. Fuel 170, 84–91. https://doi.org/10.1016/j.fuel.2015.11.086.
Xu, H., Tang, D.Z., Zhao, J.L., et al., 2015. A precise measurement method for shale porosity with low-field nuclear magnetic resonance: a case study of the Carboniferous-Permian strata in the Linxing area, eastern Ordos Basin, China. Fuel 143, 47–54. https://doi.org/10.1016/j.fuel.2014.11.034.
Xu, Y.F., Wang, Y., Yuan, H.F., et al., 2018. Pore structure characterization of tight sandstone from Sbaa Basin, Algeria: investigations using multiple fluid invasion methods. J. Nat. Gas Sci. Eng. 59, 414–426. https://doi.org/10.1016/j.jngse.2018.09.021.
Yan, W.C., Sun, J.M., Sun, Y., et al., 2018. A robust NMR method to measure porosity of low porosity rocks. Microporous Mesoporous Mater. 269, 113–117. https://doi.org/10.1016/j.micromeso.2018.02.022.
Yao, Y.B., Liu, D.M., 2012. Comparison of low-field NMR and mercury intrusion porosimetry in characterizing pore size distributions of coals. Fuel 95 (1), 152–158. https://doi.org/10.1016/j.fuel.2011.12.039.
Yao, Y.B., Liu, D.M., Xie, S.B., 2014. Quantitative characterization of methane adsorption on coal using a low-field NMR relaxation method. Int. J. Coal Geol. 131, 32–40. https://doi.org/10.1016/j.coal.2014.06.001.
Yao, Y.B., Liu, D.M., Che, Y., et al., 2010. Petrophysical characterization of coals by low-field nuclear magnetic resonance (NMR). Fuel 89 (7), 1371–1380. https://doi.org/10.1016/j.fuel.2009.11.005.
Zhang, B.N., Shan, B.C., Zhao, Y.L., et al., 2020. Review of formation and gas characteristics in shale gas reservoirs. Energies 13 (20), 5427. https://doi.org/10.3390/en13205427.
Zhao, P.Q., Cai, J.C., Huang, Z.H., et al., 2018. Estimating permeability of shale-gas reservoirs from porosity and rock compositions. Geophysics 83 (5), Mr283–Mr294. https://doi.org/10.1190/geo2018-0048.1.
Zheng, S.J., Yao, Y.B., Liu, D.M., et al., 2018. Characterizations of full-scale pore size distribution, porosity and permeability of coals: a novel methodology by nuclear magnetic resonance and fractal analysis theory. Int. J. Coal Geol. 196, 148–158. https://doi.org/10.1016/j.coal.2018.07.008.
Zhou, J., Hu, N., Xian, X., et al., 2019. Supercritical CO_2 fracking for enhanced shale gas recovery and CO_2 sequestration: results, status and future challenges. Adv. Geo-Energy Res. 3 (2), 207–224. https://doi.org/10.26804/ager.2019.02.10.